Xinjin Liu, Chunping Xie, Xuzhong Su, Heng Mei

School of Textile and Clothing,

Key Laboratory of Eco-Textile, Ministry of Education, Jiangnan University,
Wuxi 214122, P. R. China
E-mail: liuxinjin2006@163.com

Numerical Studies on a Three-dimensional Flow Field in Four-Roller Compact Spinning with a Guiding Device

Abstract
Research on the flow field in the fibre-converging zone is always the emphasis and difficulty of compact spinning. Therefore in this work numerical studies on the three-dimensional flow field in four-roller compact spinning with a guiding device were carried out using Fluent software. First a three-dimensional physical model of the fibre-converging zone was obtained using AutoCAD software. Then numerical simulations of the three-dimensional flow field in four-roller compact spinning with and without a guiding device were presented, respectively, using Fluent software. It was shown that the negative pressure is chiefly concentrated near the air-suction flume, and the velocity reaches the maximum on the centre line. Comparing with the flow field in compact spinning without a guiding device, the effective range of negative pressure in four-roller compact spinning with a guiding device increases significantly and negative pressure use efficiency improves accordingly. Furthermore the optimal installation position of the guiding device was studied, and it was shown that the optimal installation position is closely related to the linear density of the spun yarn. Finally the theoretical results obtained were illustrated by experiments.

Key words: *four-roller compact spinning, guiding device, 3D flow field, numerical simulation, fluent.*

Introduction

Compact spinning is one of the most important new kinds of spinning methods, which is implemented by adding a fibre-converging device in the front of the drafting system on a ring spinning frame. The yarn structure and quality have a qualitative development since the fibre tension distribution in the spinning triangle is more uniform [1 - 3]. Therefore research on compact spinning has attracted more and more attention and fruitful results have been achieved [4 - 8]. There are five major kinds of compact spinning at present: Rieter, Sussen, Toyota, Zinser and Roscraft, with fibre-converging in the former four being achieved by negative pressure airflow [11]. Therefore compact spinning with a negative pressure airflow fibre-converging device is the most extensive at present, with research on the flow field in the fibre-converging zone always being the emphasis and difficulty of this kind of compact spinning [6 - 8]. Four-roller compact spinning with a negative pressure airflow fibre-converging device is the most widely used, which accounts for about 70%, and occupies the leading position on the market. Therefore the aim of this paper was to perform numerical studies on the three-dimensional flow field in four-roller compact spinning with a guiding device using Fluent software, and lay the foundation for system optimisation.

The traditional theoretical analysis method, experimental measurement method and computational fluid dynamics method comprise a complete system for studying the flow field [9]. Especially the computational fluid dynamics method has become the most powerful tool for studying the flow field at present [7, 8], with Fluent being one of the most generally used software accordingly [10]. Fruitful results for the flow field have been obtained by using Fluent software [6 - 8]. For example, the airflow velocity in the condensing zone of compact spinning with a perforated drum was extracted by Fluent 6.3.26 software, and a dynamic model for simulating the fibre motion trajectory in the condensing zone was constructed and solved by a specially designed MATLAB program [6]. A computational fluid dynamic model, computed with parallel technologies and Fluent 6.3, was developed to simulate the flow field in the compact zone with 3D

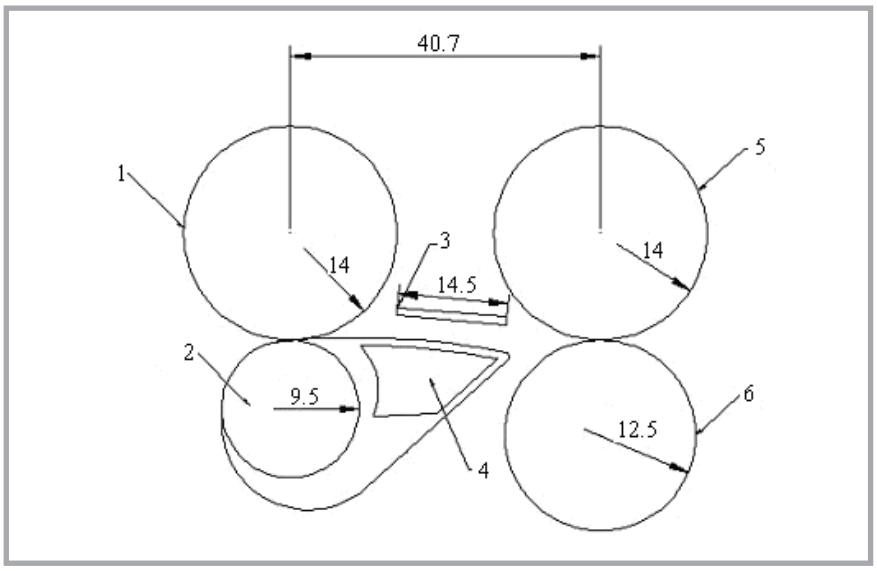

Figure 1. *The fibre-converging zone in four-roller compact spinning with guiding device; 1) output top roller, 2) air-suction flume, 3) guiding device, 4) shaped tube, 5) drafting top roller, 6) front roller.*

Liu X, Xie C, Su X, Mei H. Numerical Studies on a Three-dimensional Flow Field in Four-Roller Compact Spinning with a Guiding Device. *FIBRES & TEXTILES in Eastern Europe* 2013; 21, 6(102): 50-57.

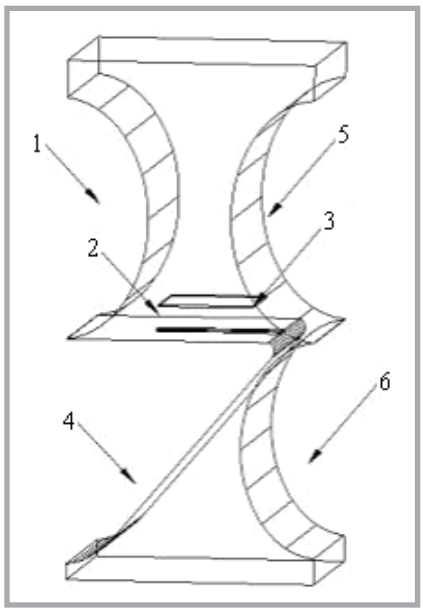

Figure 2. *A three-dimensional physical model of fibre-converging zone.*

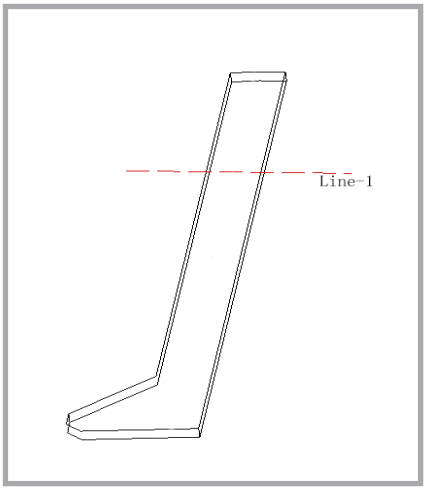

Figure 3. *The structure of the Air-Suction Flume.*

computational fluid dynamic technology for compact spinning with an inspiratory groove [7], and so on. However, researches on the flow field in four-roller compact spinning have not been found until now. The guiding device is an effective equipment installed in the fibre-converging zone which can improve the use efficiency of airflow. Rieter's COM4 system is equipped with a guiding device. Motivated by all these research works above, this work attempts to investigate the Three-dimensional flow field in four-roller compact spinning with a guiding device. The three-dimensional flow field of four-roller compact spinning with a guiding device was investigated by using Fluent software. First, according to the physical parameters of the practical four-roller compact spinning system measured, a three-dimensional physical model of the condensing zone was obtained using AutoCAD software. Secondly the boundary conditions and turbulence model used in the simulations were attained. Thirdly according to the physical model, boundary conditions and turbulence model, by using fluent software, numerical simulation results of the flow velocity in three cross sections were presented. In the simulation results how the airflow flows in three cross sections can be seen, and then we can establish how the airflow acts on fibres in the condensing zone. Moreover the magnitude of negative pressure can also be observed, which lays the foundation for system optimisation. The effectiveness of the guiding device for improving the use efficiency of negative pressure airflow was emphasised, and the optimal installation position of the guiding device was studied.

Three-dimensional physical model of fibre-converging zone

The selective fibre-converging zone in four-roller compact spinning with a guiding device is shown in ***Figure 1***, the parameters of which are measured directly according to practical four-roller compact spinning. Then a three-dimensional physical model for the fibre-converging zone can be obtained using AutoCAD software (see ***Figure 2***). In this model, two simplifying assumptions were made: Firstly the fibre strand is ignored since its volume is much smaller than that of fibre-converging zone. Secondly the lattice apron is also ignored for convenience of numerical simulation. We also suppose that the output direction of the fibre strand is the x-axis, the transverse converging direction of the fibre strand is the y-axis, and the thickness direction of the fibre strand is the z-axis. For convenience of subsequent comparative analyse, a straight line 1 is defined in the flow field, which is parallel to the y-axis, and clings to the surface of the air-suction flume (see ***Figure 3***).

Numerical simulation of three-dimensional flow field using Fluent

Setting boundary conditions

The airflow in the fibre-converging zone is considered as incompressible and satisfies Reynolds equations. The turbulence model adopts the k - ε two-equation model. According to the physical model, the bottom surface of the air-suction flume is set as the pressure outlet boundary; the superior surface and side of the shaped tube is set as the pressure outlet boundary and other surfaces are set as the wall. The detail boundaries are set as follows:

1) Pressure outlet boundary: temperature - 298K, pressure - standard atmosphere.
2) Pressure inlet boundary: presupposition, k, ε are free variables.
   Here, $k = (c\% \times v^2)/2$,
   $\varepsilon = (c\% \times k^{3/2})/0.03$, $c = 0.5 \sim 1.5$.
3) Wall boundary: non-slip boundary conditions.

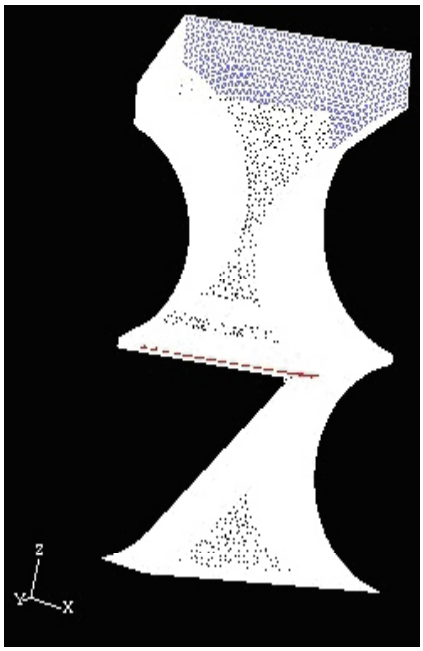

Figure 4. *The mesh generation of physical model.*

Mesh generation and calculation method setting

Mesh generation of the three-dimensional physical model can be obtained using Gambit software (see ***Figure 4***), in which general unstructured quadrilateral mesh generation methods are adopted, with the computing units being 467423.

The calculation methods are set as follows: Solvers - Single Precision Implicit Split-Operator, Discretisation scheme - First Order Upwind Difference Scheme, Coupling problem between pressure and velocity - SIMPLE Algorithm, Viscosity Coefficient and Density on Interface--Arithmetic mean of adjacent nodes.

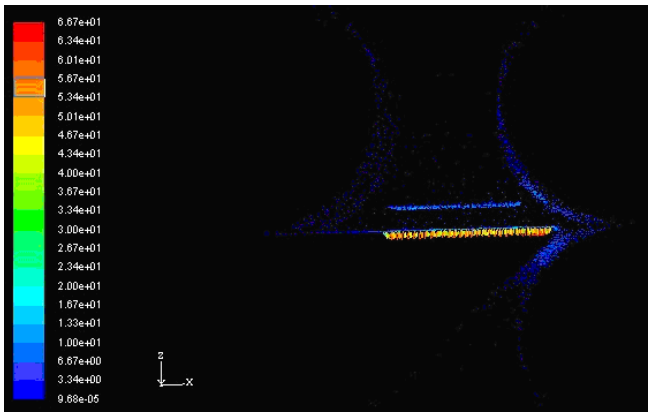

Figure 5. *The vector diagram of flow velocity in fiber-converging zone.*

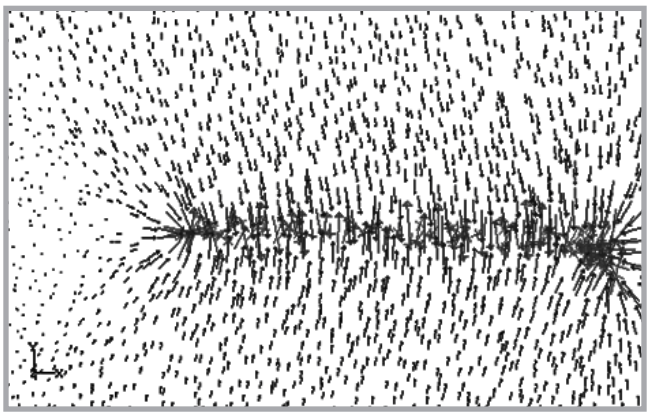

Figure 6. *The vector diagram of flow velocity in X-Z cross section.*

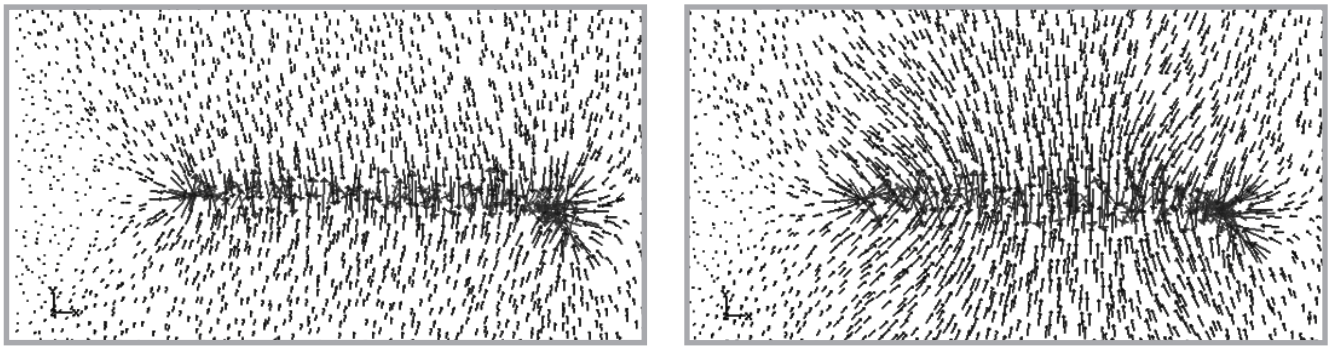

Figure 7. *The vector diagram of flow velocity in X-Y cross section; a) without, b) with guiding device.*

Numerical simulation results - flow velocity

By using Fluent software, all the numerical simulation results of flow velocity are shown in ***Figure 5***, and a corresponding vector diagram on the X-Z section (forward direction of fibre strands) is shown in ***Figure 6***. It is shown that the effective range of negative pressure is mainly concentrated in the zone near the air-suction flume, and the streamline density of the flow velocity reaches the maximum in the air-suction flume, with the flow velocity also reaching the maximum accordingly. For illustrating the effects of the guiding device on the flow field distribution in the fibre-converging zone, corresponding vector diagrams of flow velocity with and without a guiding device on the X-Y section (converging direction of fibre strands) are shown in ***Figure 7***. It is obvious that the streamline density of flow velocity in the fibre-converging zone of compact spinning with a guiding device increases significantly, with the flow velocity also increasing accordingly. The effective range of negative pressure also rises, which is beneficial for improving the fibre compacting effect. Furthermore vector diagrams of the flow velocity with and without guiding device above Line 1 are shown in ***Figure 8***. Here distance d between the guiding device and lattice apron is equal to 3 mm. In the Figures, the abscissa point $y = 0.018$ represents the center point of the air-suction flume, with the positive value showing that the velocity direction is consistent with the positive direction of the corresponding axis, whereas the negative value is consistent with the negative direction of the corresponding axis.

The flow velocity component on X direction (output direction of fibre strand) is shown in ***Figure 8.a***, which mainly affects the transportation of fibre strands. It is obviously that the component in the X direction with a guiding device increases more significantly than that without a guiding device, and the fluctuation is smaller, i.e. flow stability is better, which is beneficial for improving yarn evenness. The flow velocity component in the Y direction (transverse converging direction of fibre strand) is shown in ***Figure 8.b***, which mainly affects fibres converging. It is shown that the flow velocity components on the left and right sides of the air-suction flume are opposites. The nearer to the air-suction flume, the larger the flow velocity component in this direction. It is obvious that the component in the Y direction with a guiding device also increases more significantly than that without a guiding device, with the continuity of the flow velocity streamline also being better, which is consistent with ***Figure 7***. According to kinetic energy equation $E = 0.5mv$, we know that when the quality of fibre strand m is constant, the larger the flow velocity v is, the larger kinetic energy E is, which is beneficial for improving fibre covering during spinning. The flow velocity component in the Z direction (thickness direction of fibre strand) is shown in ***Figure 8.c***, which mainly makes the fibre strands cling to the lattice apron, and prevents the dispersion of fibre strands. It is obvious that the component in the Z direction with a guiding device is almost the same as that without a guiding device.

Numerical simulation results - static pressure

By using Fluent software, numerical simulation results of static pressure are shown in ***Figure 9***. It is seen that the static pressure near the air-suction flume is negative and becomes positive gradually far away from the air-suction flume, until equal to standard atmosphere.

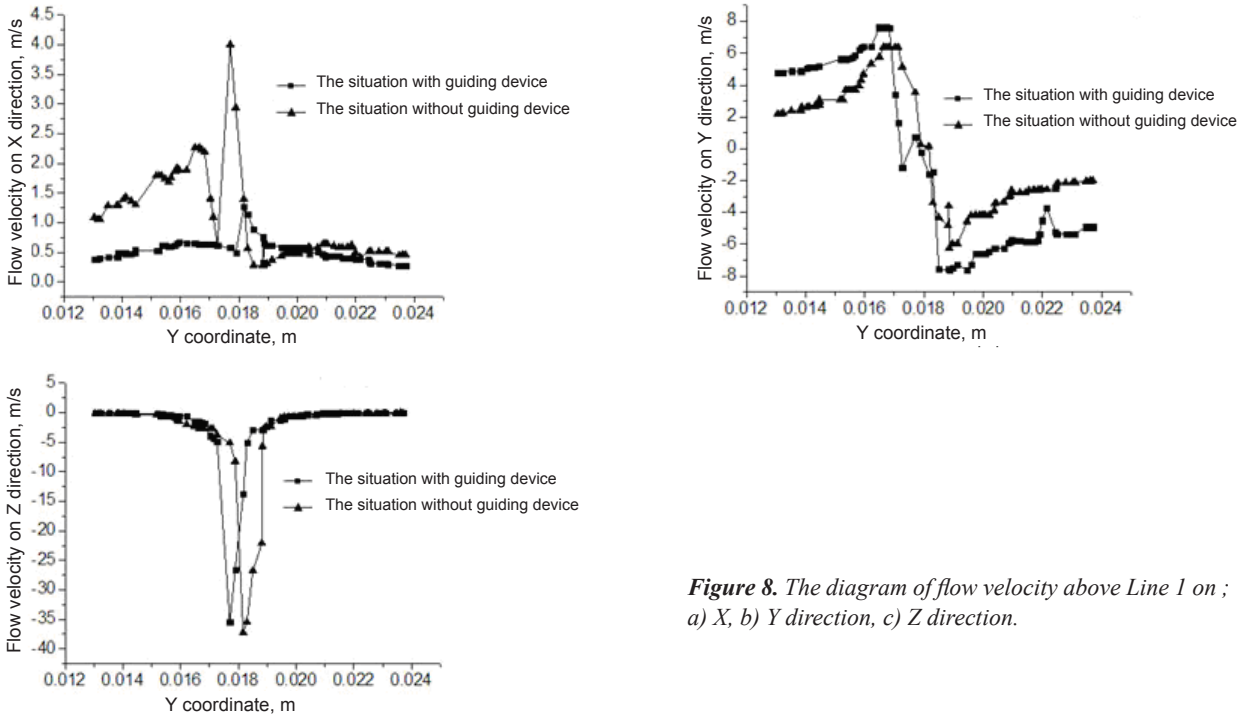

Figure 8. *The diagram of flow velocity above Line 1 on ; a) X, b) Y direction, c) Z direction.*

For illustrating the effects of the guiding device, corresponding vector diagrams of static pressure with and without a guiding device above Line 1 are shown in ***Figure 10***. It is obvious that static pressure reaches the maximum at the centerline of the air-suction flume (y = 0.018), which makes the fibre in the spinning triangle gather to the centerline easily, and the spinning triangle decreases accordingly, beneficial for uniform fibre tension distributions in the spinning triangle. Meanwhile it is shown that the maximum value of static pressure in the fibre-converging zone with a guiding device is -1,800 Pa, while it is -1,600 Pa without one, i.e. an effective improvement of 12.5% due to the installation of a guiding device. Furthermore the variation in airflow is stable with a guiding device, which is beneficial for improving negative pressure use efficiency and yarn evenness.

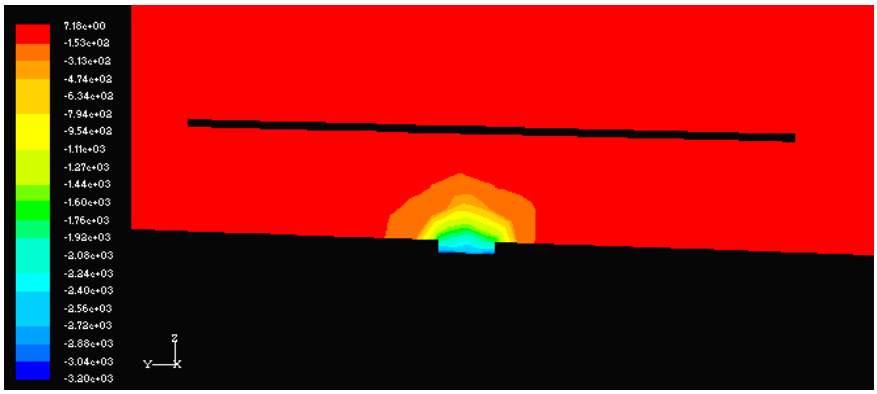

Figure 9. *The vector diagram of static pressure in fiber-converging zone.*

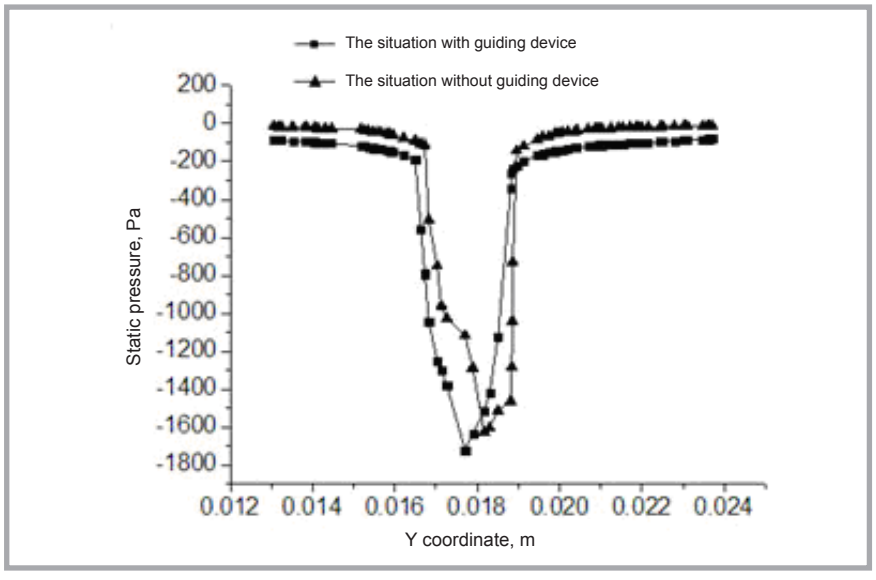

Figure 10. *The diagram of static pressure above Line 1.*

Installation position of guiding device optimisation

Effect of different installation positions on flow velocity

In this section, the effects of distance d between the guiding device and lattice apron on flow field distributions in the fibre-converging zone will be discussed. Three different distances d = 3, 4, 5 mm are discussed, respectively. By using Flu-

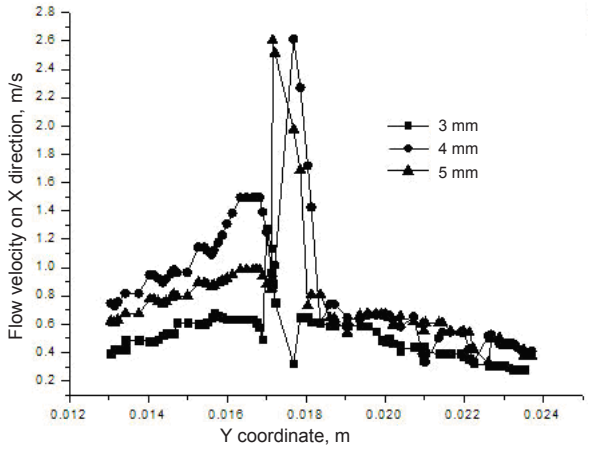

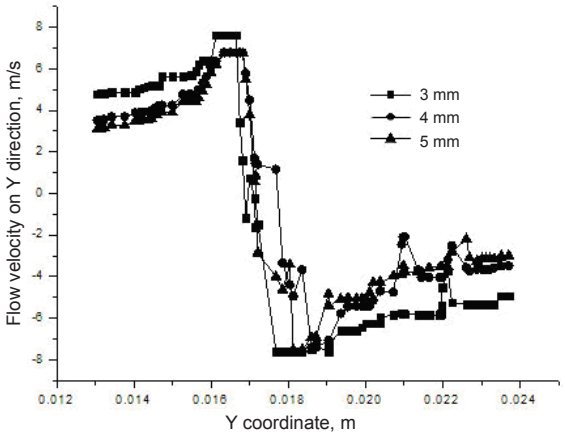

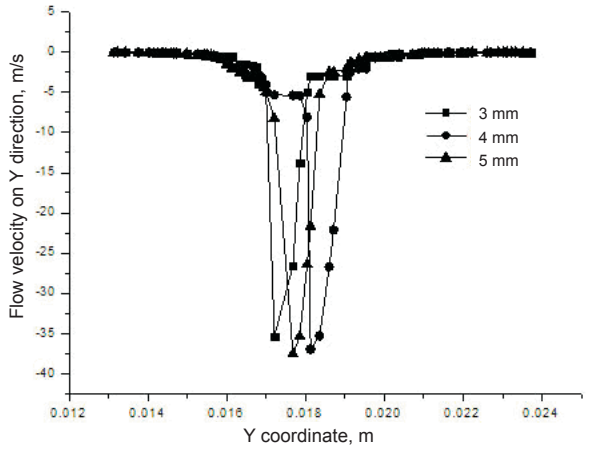

Figure 11. *The diagram of flow velocity above Line 1 with different guiding device position: The flow velocity on; a) X, b) Y, c) Z direction.*

ent software, vector diagrams of the flow velocity above line 1 are shown in ***Figure 11***.

The flow velocity component in the *X* direction (output direction of fibre strand) is shown in ***Figure 11.a***. It is obvious that the component in the *X* direction with $d = 3$ mm is smaller than that of $d = 4$ mm and $d = 5$ mm, with the fluctuation also being smaller, i.e. the flow stability is better, which is beneficial for improving yarn evenness. Airflow in this direction mainly affects the transportation of fibre strands. From this point, the larger the distance, the better the effect of fibre compacting. The flow velocity component in the *Y* direction (transverse converging direction of the fibre strand) is shown in ***Figure 11.b***. It is obvious that the component in the *Y* direction with $d = 3$ mm is larger than that of $d = 4$ mm and $d = 5$ mm, with the fluctuation being smaller, which is beneficial for improving fibre compacting. The flow velocity component in the *Z* direction (thickness direction of the fibre strand) is shown in ***Figure 11.c***. On the one hand, the flow velocity component on this direction makes the fibre strands cling to the lattice apron and prevents the dispersion of fibre strands, while on the other, the friction between the fibre strand and lattice apron will be produced under this airflow force, which is unfavorable for fibre covering. The flow velocity in this direction increases with an increase in distances *d*. From this point, the flow velocity component in this direction should be suitable, with the smaller distance being appropriate for yarn spinning with low linear density, while the larger distance is suitable for yarn spinning with high linear density.

Effect of different installation positions on static pressure

The contour of static pressures on the X-Y section (converging direction of fibre strands) is shown in ***Figure 12***, and corresponding vector diagrams above Line 1 are shown in ***Figure 13*** with three different distances *d*. It is shown that the effective range of negative pressure in-

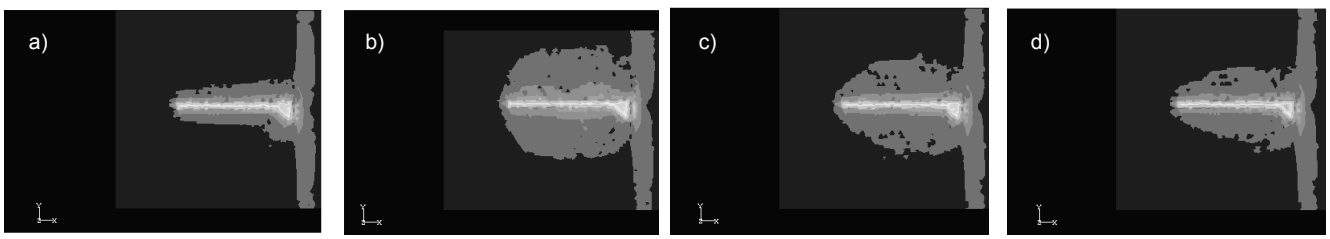

Figure 12. *Vector diagrams of static pressure above Line 1 with different guiding device positions; a) static pressure without guiding device, b) d = 3 mm, c) d = 4 mm, d) d = 5 mm*

creases significantly with the help of the guiding device comparing ***Figure 12.a*** with ***Figure 12.b***, which is beneficial for transverse converging and prevents fibre diffusion. At the same time, the end of the air-suction flume in the four-roller compact spinning system cannot extend to the nip, i.e. there is no compacting effect in the distance between the end of the air-suction flume and the nip. The existence of the guiding device can make up for this defect. Comparing ***Figure 12.b, 12.c*** and ***12.d***, the effective range of negative pressure increases with a decrease in distance *d*. However, too small distance may make the fibre strand hit the lattice apron and cause yarn evenness deterioration, i.e. the optimal guiding device installation position is closely related to spun yarn linear density, which is verified in the next section.

Experiments

In this section the conclusions obtained in the previous section were verified by experiments. The material of the guiding device used in this paper is organic glass plate, which was rectangular, length 60 mm and width 15.4 mm. The plate was divided into two sections: A - upper end of air-suction flume (36 mm), B - fixed part (24 mm) (see ***Figure 14***).

Effects of guiding device on yarn qualities

In this section, the effects of the guiding device on yarn qualities were verified by experiments. Three different kinds of yarn were spun: 7.3 tex, 9.7 tex, 14.6 tex on a spinning frame EJM128K. Details of the spinning parameters are shown in ***Table 1***. The test instruments were as follows: single yarn tester YG063, hairiness tester YG172A, evenness tester YG135G.

The higher breaking strengths and less hairiness of the spun yarns are the key achievements of compact spinning technology. Therefore 3 ~ 9 mm hairiness, breaking strength and evenness of the spun yarn were measured, the results of which are given in ***Table 2***. Here $d = 0$ represents the case without a guiding device. From ***Table 2***, it is obvious that all the qualities of spun yarn measured with a guiding device are better than without one. For spun yarn with a guiding device, the comprehensive qualities are best for 14.6 tex yarn with $d = 5$ mm, 9.7 tex yarn with $d = 3$ mm, and 7.3 tex yarn with

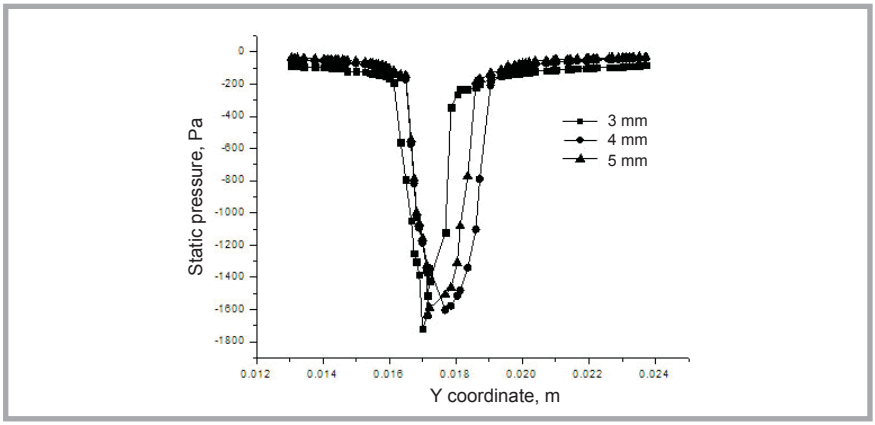

Figure 13. *The diagram of static pressure above Line 1 with different guiding device positions.*

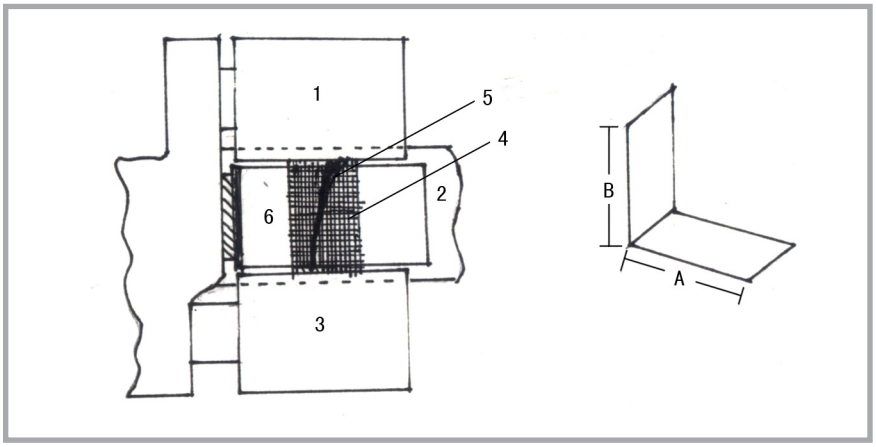

Figure 14. *The installation diagram of guiding device; 1) Drafting top roller, 2) Shaped tube, 3) Output top roller, 4) Lattice apron, 5) Air-suction flume, 6) Guiding device.*

Table 1. *Spinning parameters.*

Linear density, tex	Roving feeding, g·(10 m)$^{-1}$	Twist, t.p.m.	Front roller speed, r·min^{-1}	Spacer, mm	Negative pressure, Pa	Traveller
14.6	4.25	932.6	222	2.8	2800	8/0
9.7	3.00	1259.4	178	2.7	2800	10/0
7.3	3.00	1406.4	159	2.5	2800	11/0

Table 2. *Testing results of yarn qualities.*

Linear density, tex	Installation position of guiding device (d), mm	Testing index		
		Breaking strength, cN	Evenness, CV%	Hairiness (3 mm), (10 m)$^{-1}$
14.6	0	266.9	13.78	7.2
	3	270.5	13.47	6.5
	4	276.8	13.36	5.8
	5	276.4	13.13	5.2
9.7	0	183.5	12.99	7.2
	3	185.2	12.85	5.8
	4	191.3	12.23	5.1
	5	187.6	12.15	5.3
7.3	0	126.3	12.95	5.7
	3	135.2	12.12	3.9
	4	129.6	12.63	4.1
	5	127.0	12.74	4.6

Table 3. Spinning parameters.

Linear density, tex	Roving feeding, g·(10 m) $^{-1}$	Twist, t.p.m.	Front roller speed, r·min^{-1}	Spacer, mm	Guiding device position (d), mm
14.6	4.25	932.6	222	3.0	5
9.7	3.00	1259.4	178	2.8	4
7.3	3.00	1406.4	159	2.5	3

d = 3 mm, respectively, which shows that the optimal guiding device installation position is closely related to spun yarn linear density.

In the following, the effects of the guiding device on spinning system energy consumption were verified by experiments. Three different kinds of yarn were spun: 7.3 tex, 9.7 tex & 14.6 tex on a spinning frame EJM128K with different converter frequencies. Details of spinning parameters are shown in ***Table 3***. The measuring results are given in ***Table 4***, from which it is obvious that the negative pressure and flow velocity in the fibre-converging zone with a guiding device are larger than without a guiding device for the same converter frequency, i.e. the fibre compacting effect is better. Corresponding three qualities of spun yarn are shown in ***Table 5***. It is also seen that all measuring qualities of spun yarn with a guiding device are better than without a guiding device.

Summary

In this paper, numerical studies on a three-dimensional flow field in four-roller compact spinning with a guiding device were investigated by using Fluent software. Using AutoCAD software, a three-dimensional physical model of the fibre-converging zone was obtained according to the parameters of practical four-roller compact spinning measured. Numerical simulation of the three-dimensional flow field in four-roller compact spinning with and without a guiding device has been presented, respectively, using Fluent software. It is shown that the negative pressure is chiefly concentrated near the air-suction flume, with the velocity reaching the maximum on the center line. The effective range of negative pressure in four-roller compact spinning with a guiding device increases significantly and the use efficiency of negative pressure improves accordingly. Furthermore the effects of distance d between the guiding device and lattice apron on yarn qualities have been discussed. It is shown that the optimal guiding device installation position is closely related to spun yarn linear density. The theoretical results obtained in this paper were finally illustrated by experiments.

Table 4. Testing results of spinning system energy.

Linear density, tex	Number	Converter frequency, Hz	Negative pressure value without guiding device, Pa	Flow velocity without guiding device, m·s^{-1}	Negative pressure value with guiding device, Pa	Flow velocity with guiding device, m·s^{-1}
14.6	1	185	2607	4.36	2631	5.06
	2	195	2801	5.08	2825	5.76
	3	205	3003	5.73	3031	6.53
9.7	4	185	2600	4.42	2641	5.66
	5	195	2796	5.12	2843	6.50
	6	205	3011	5.65	3059	7.23
7.3	7	175	2402	3.61	2488	5.90
	8	185	2604	4.31	2697	7.03
	9	195	2803	5.10	2906	8.26
	10	205	2999	5.84	3106	9.52

Table 5. Testing results of yarn qualities.

Number	Guiding device (Yes or No)	Breaking strength, cN	Evenness, CV%	Hairiness (3 mm),·(10 m)$^{-1}$
1	No	254.8	14.12	8.5
	Yes	267.9	13.76	6.9
2	No	266.4	13.82	7.1
	Yes	276.1	13.15	5.3
3	No	277.6	13.17	5.7
	Yes	284.4	13.04	4.6
4	No	172.9	13.45	7.8
	Yes	187.6	12.63	6.4
5	No	180.5	13.04	7.2
	Yes	198.6	12.16	5.4
6	No	188.2	12.56	6.1
	Yes	210.4	12.04	4.7
7	No	120.9	13.14	6.7
	Yes	135.3	12.36	4.8
8	No	126.3	12.95	5.7
	Yes	141.6	12.09	3.8
9	No	131.5	12.67	4.3
	Yes	145.7	11.04	2.9
10	No	135.2	12.25	4.6
	Yes	127.6	12.54	2.5

Acknowledgements

This work was supported by the National Natural Science Foundation of P. R. China under Grant 11102072, the Fundamental Research Funds for the Central Universities JUSRP21104, the Natural Science Foundation of Jiangsu Province under Grant BK2012254, Prospective industry-university-research project of Jiangsu Province (BY2011117, BY2012065) and a Project Funded by the Priority Academic Program Development of Jiangsu Higher Education Institutions.

References

1. Skenderi Z, Vitez D. Compact spinning - A new chance for ring spinning. *TEKSTIL* 2003; 52, 1: 11-17.
2. Cheng KPS, Yu C. A study of compact spun yarns. *Textile Research Journal* 2003; 73, 4: 345-349.
3. Nikolic M, Stjepanovic Z, Lesjak F, Stritof A. Compact spinning for improved quality of ring-spun yarns. *Fibres & Textile in Eastern Europe* 2003; 11, 4: 30-35.
4. Dou HP, Liu SR. Trajectories of fibers and analysis of yarn quality for compact spinning with pneumatic groove. *Journal of the Textile Institute* 2011; 102, 8: 713-718.
5. Xu BJ, Ma J. Radial Distribution of Fibres in Compact-Spun Flax-Cotton Blended Yarns. *Fibres & Textiles in Eastern Europe* 2010; 18, 1: 24-27.
6. Zou ZY, Cheng LD, Hua ZH. A Numerical Approach to Simulate Fiber Motion Trajectory in an Airflow Field in Compact Spinning with a Perforated Drum. *Textile Research Journal* 2010; 80, 5: 395-402.
7. Zhang XC, Zou ZY, Cheng LD. Numerical Study of the Three-dimensional Flow Field in Compact Spinning with Inspiratory Groove. *Textile Research Journal* 2010; 80, 1: 84-92.
8. Fu PH, Cheng LD. Numerical Simulation for the Pneumatic Compacting Field in Compact Spun Technology. In: Asia *Simulation System Simulation Conference 2005. The Six International Conference on and Scientific Computing*. 10: 432, 2005.
9. Zhou JJ. FLUNT engineering and example analysis. Beijing: China Water Conservancy and Hydropower, 2010.
10. Chen GL, Li GW, Guo YB, Wang Q. A Simulation Study of Concentration Basin in hydrodynamics with Fluent Software. *Research Journal of Chemistry and Environment* 2011; 15, 2: 504-509.
11. Li MF. Simple Analyses of Structure of Compact Spinning Set. *Cotton Textile Technology* 2003; 31, 10: 591-595.

Received 20.08.2012 Reviewed 14.02.2013